Available online at www.sciencedirect.com
SCIENCE DIRECT®
Journal of Sound and Vibration 292 (2006) 519–534
JOURNAL OF SOUND AND VIBRATION
www.elsevier.com/locate/jsvi

Investigation of damping and radiation using full plane wave decomposition in ducts

Sabry Allam, Mats Åbom*

The Marcus Wallenberg Laboratory for Sound and Vibration Research, Department of Aeronautical and Vehicle Engineering, KTH, SE-10044 Stockholm, Sweden

Received 4 January 2005; received in revised form 1 June 2005; accepted 9 August 2005
Available online 2 November 2005

Abstract

A general plane wave decomposition procedure that determines both the wave amplitudes (or the reflection coefficient) and the wavenumbers is proposed for in-duct measurements. To improve the quality of the procedure, overdetermination and a nonlinear least-squares procedure is used. The procedure has been tested using a six microphone array, and used for accurate measurements of the radiation from an open unflanged pipe with flow. The experimental results for the reflection coefficient magnitude and the end correction have been compared with the theory of Munt. The agreement is very good if the maximum speed rather than the average is used to compare measurements and theory. This result is the first complete experimental validation of the theory of Munt [Acoustic transmission properties of a jet pipe with subsonic jet flow, I: the cold jet reflection coefficient, *Journal of Sound and Vibration* 142(3) (1990) 413–436]. The damping of the plane wave (the imaginary part of the wavenumber) could also be obtained from the experimental data. It is found that the damping increases strongly, compared with the damping for a quiescent fluid, when the acoustic boundary layer becomes thicker than the viscous sublayer. This finding is in agreement with a few earlier measurements and is also in agreement with a theoretical model proposed by Howe [The damping of sound by wall turbulent sheer layers, *Journal of Acoustic Society of America* 98(3) (1995) 1723–1730]. The results reported here are the first experimental verifications of Howe's model. It is found that the model works well typically up to a normalized acoustic boundary layer thickness δ_A^+ of 30–40. For values of a δ_A^+ less than 10, corresponding to higher frequencies or lower flow speeds, the model proposed by Dokumaci [A note on transmission of sound in a wide pipe with mean flow and viscothermal attenuation, *Journal of Sound and Vibration* 208(4) (1997) 653–655] is also in good agreement with the experimental data.

1. Introduction

1.1. General

There are two standards methods for measuring in-duct acoustic properties; the standing wave ratio (SWR) and the two-microphone method (TMM) [1,2]. Although the SWR method can yield accurate results in a stationary medium, it is very time consuming; especially in measuring the acoustic properties for a wide

*Corresponding author. Tel.: +46 8 790 7944; fax: +46 8 790 6122.
E-mail address: matsabom@kth.se (M. Åbom).

0022-460X/$ - see front matter © 2005 Elsevier Ltd. All rights reserved.
doi:10.1016/j.jsv.2005.08.016

frequency range with a linear frequency step and it is difficult to apply in a turbulent mean flow [3]. By using the TMM with broadband excitation, acoustic properties can be determined over a very wide frequency range and the measurement can be much faster than with the SWR method. However, to accurately cover sufficiently large frequency ranges with a desired accuracy normally more than one microphone spacing is needed [4,5]. Many works have been devoted to the analysis of the accuracy of the TMM [6–11]. Fujimori et al. [12] introduced the least-squares method based on the data sampled at multiple measurement points, and Pope [13] showed that the least-squares method using broadband excitation and the transfer function between two measuring points is actually equivalent to the TMM. Chu [4,5] reported that the least-squares method gives more accurate results than the TMM if the measurement is performed at multiple points. However, the measuring sensor positions were chosen arbitrarily in his work and no guideline based on an analytical investigation has been given. Jones and Parrott [14] suggested a multi-point method using least-squares estimation with pure tone excitation. Seung-Ho et al. [15] showed that improved measurement results can be obtained by adopting additional measurement points evenly spaced within half a wavelength and using the least-squares method with broad-band excitation.

All the previous works presented and summarized above suggest that the complex wavenumbers $k_{\pm}$ are known, based on theoretical or empirical formulas [16–21]. For the case with no flow and a duct where wall vibrations can be neglected, the wavenumber for circular cross-sections can be calculated from the Kirchhoff solution for plane waves in a thermo-viscous fluid [22]. With a mean flow the situation is more complex and no complete theory exists [16–21].

Investigations of plane wave damping in ducts have been carried out, for instance, by Ronneberger and Ahrens [23] and Peters et al. [24]. Ronneberger and Ahrens [23] used 10 microphones and a regression analysis to measure the wavenumbers in a turbulent pipe flow. The damping investigation was done at two fixed frequencies at varying flow Mach numbers. The full plane wave decomposition method described in this paper is similar to the method proposed by Ronneberger and Ahrens [23]. But while the latter is tailor-made for the measurement of wave damping, the procedure described here allows simultaneous determination of both wave amplitudes and wavenumbers. Based on the two-microphone theory Peters et al. [24] used two different clusters of microphones to pick up the in-duct data at low frequencies up to Mach numbers $M \leqslant 0.1$. By applying the standard TMM and neglecting damping between the microphones, the complex reflection coefficient can be calculated for each cluster. By comparing the two values of the reflection coefficient at the two clusters and taking into account the distance between the clusters (4.165 m), the wave damping can be calculated.

The underlying motivation for this study was the wish to accurately measure the reflection from an open ended pipe with flow. In particular, to validate the famous theoretical model by Munt [25] for this problem. Preliminary tests using the classical TMM showed that in particular the phase of the reflection coefficient, which also can be represented as an end-correction, was difficult to measure. To minimize the effect of errors it was therefore decided to use a multi-microphone arrangement and overdetermination. However, since the wavenumber in particular the imaginary part associated with the damping is not accurately known in a flow duct it was decided to also include the wavenumber as an unknown. This led to the development of the full plane wave decomposition procedure which will be described below. As a bonus the accurate measurements of the reflection coefficient also gave new empirical data for the damping in a duct. These data were used to test some of the theories and models for damping of plane waves in ducts which has been published.

1.2. Theory of the two-microphone method

In every straight cylindrical duct the sound field below the first cut-on frequency will consist only of plane waves. In the frequency domain, the sound field can then be written as

$$\hat{p}(x,f) = \hat{p}_+(f)\exp(-\mathrm{i}k_+x) + \hat{p}_-(f)\exp(\mathrm{i}k_-x),$$
$$\hat{u}(x,f) = \frac{1}{\rho c}\left[\hat{p}_+(f)\exp(-\mathrm{i}k_+x) - \hat{p}_-(f)\exp(\mathrm{i}k_-x)\right], \quad (1)$$

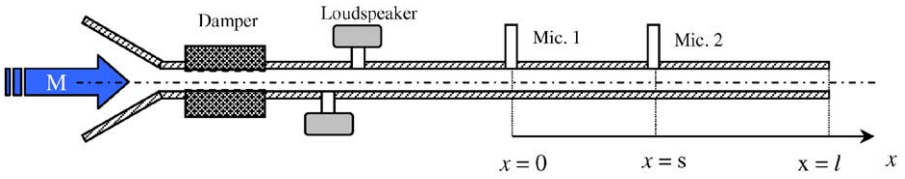

Fig. 1. Measurement configuration for the TMM.

where $\hat{p}$ is the Fourier transform of the acoustic pressure, $\hat{u}$ is the Fourier transform of the particle velocity, x is the coordinate along the duct axis, f is the frequency, k is the complex wavenumber $\pm$ denotes propagation in positive and negative x-direction, ρ is the density and c is the speed of sound.

By assuming the complex wavenumbers are known in the duct, the incident and reflected wave amplitudes $\hat{p}_+$ and $\hat{p}_-$ can be calculated using two microphone positions as shown in Fig. 1.

$$\hat{p}_1 = \hat{p}_+(f) + \hat{p}_-(f), \tag{2}$$

$$\hat{p}_2 = \hat{p}_+(f)\exp(-\mathrm{i}k_+ s) + \hat{p}_-(f)\exp(\mathrm{i}k_- s), \tag{3}$$

where s represents the microphone separation. Eqs. (2) and (3) imply that

$$\hat{p}_+(f) = \frac{\hat{p}_1(f)\exp(\mathrm{i}k_- s) - \hat{p}_2(f)}{\exp(\mathrm{i}k_- s) - \exp(-\mathrm{i}k_+ s)}, \tag{4}$$

$$\hat{p}_-(f) = \frac{-\hat{p}_1(f)\exp(-\mathrm{i}k_+ s) + \hat{p}_2(f)}{\exp(\mathrm{i}k_- s) - \exp(-\mathrm{i}k_+ s)}. \tag{5}$$

Eqs. (4) and (5) are the basic TMM equations from which all plane wave quantities of interest can be calculated. To use these equations in practice it is firstly necessary to compensate for the amplitude and phase shift associated with each microphone channel. Secondly, with flow in the duct it is necessary to improve the signal-to-noise ratio by using the source signal (loudspeaker voltage) as a reference. If we assume that the duct has a linear and passive termination in the postive x-direction a reflection coefficient can be defined in that direction

$$R(f) = \frac{\hat{p}_-}{\hat{p}_+}. \tag{6}$$

Bodén and Åbom [8] proved that the TMM has its lowest sensitivity to errors in the input data in a region around $ks = \pi(1 - M^2)/2$, where M is the Mach number. Also Åbom and Bodén [9] suggested that to avoid a large sensitivity to errors in the input data, the TMM should be restricted to the frequency range.

$$0.1\pi\left(1 - M^2\right) < ks < 0.8\pi\left(1 - M^2\right). \tag{7}$$

2. Theory of the full wave decomposition method (FWDM)

Based on the measured data at N microphone positions an overdetermined nonlinear solver has been introduced and used to predict the full in-duct acoustic properties, i.e., complex wave amplitudes $\hat{p}_\pm$ and wavenumbers $k_\pm$. The sound field at the N microphones can be represented using Eq. (1) as

$$\hat{p}_j = \hat{p}_+(f)\exp(-\mathrm{i}k_+ x_J) + \hat{p}_-(f)\exp(\mathrm{i}k_- x_J), \tag{8}$$

where $J = 1, 2, \ldots, N$ is the microphone position and $\pm$ denote propagation in positive and negative x-direction. To solve for the four unknowns at least 4 microphone positions are needed and to obtain an overdetermined problem we must choose $N > 4$.

Concerning the choice of the positions there are different strategies. One being the use of a uniform distribution over a distance corresponding to half a wavelength at the lowest frequency of interest as suggested by Seung-Ho et al. [15]. This alternative is the best if only estimates of reflection coefficients and wave amplitudes are of interest. If we also are interested in obtaining accurate data for the wavenumbers

arrangements where the microphones are split into two clusters (half in each), separated by a sufficiently long distance to produce a measurable effect of the wave damping, seems to be a logical choice [24].

2.1. Solution procedure

Based on Eq. (8) and combining the theoretical wave representation and measured data at each microphone position with $N>4$, an overdetermined nonlinear system of equations is obtained

$$(F_J) = (A_J) - (B_J) = 0, \tag{9}$$

where

$$(A_J) = \left(\hat{p}_+ \exp(-\mathrm{i}k_+x_J) + \hat{p}_- \exp(\mathrm{i}k_-x_J)\right),\ (B_J) = \left(\hat{p}_J\right). \tag{10}$$

Here $(F_J(\mathbf{y})) = 0$ is an equation in C^N which has to be solved to get the unknown $\mathbf{y} = \left[\hat{p}_+\ k_+\ \hat{p}_-\ k_-\right]^{\mathrm{T}}$. There are several methods that can be used to solve an overdetermined nonlinear system of equations [26]. Here a damped Gauss–Newton iterative procedure is used which implies

$$\mathbf{y}_{n+1} = \mathbf{y}_n - \lambda \mathbf{d}(\mathbf{y}_n). \tag{11}$$

The search direction can be calculated using the Gauss–Newton method $\mathbf{d}(\mathbf{y}) = \left((DF_J)^{\mathrm{T}}DF_J\right)^{-1}(DF_J)^{\mathrm{T}}(F_J)$, where

$$DF_J = \begin{bmatrix} \dfrac{\partial F_J}{\partial \hat{p}_+} & \dfrac{\partial F_J}{\partial k_+} & \dfrac{\partial F_J}{\partial \hat{p}_-} & \dfrac{\partial F_J}{\partial k_+} \end{bmatrix}. \tag{12}$$

The derivatives are found using Eq. (10)

$$\begin{aligned} \frac{\partial F_J}{\partial \hat{p}_+} &= \exp(-\mathrm{i}k_+x_J), & \frac{\partial F_J}{\partial k_+} &= \hat{p}_+(-\mathrm{i}x_J)\exp(-\mathrm{i}k_+x_J), \\ \frac{\partial F_J}{\partial \hat{p}_-} &= \exp(\mathrm{i}k_-x_J), & \frac{\partial F_J}{\partial k_-} &= \hat{p}_-(\mathrm{i}x_J)\exp(\mathrm{i}k_-x_J). \end{aligned} \tag{13}$$

The damping factor λ is initially put equal to 1, but if $F(\mathbf{y}_n - \lambda\mathbf{d}_n) \geqslant F(\mathbf{y}_n)$, then λ is halved. This is repeated until $F(\mathbf{y}_n - \lambda\mathbf{d}_n) < F(\mathbf{y}_n)$ and the same procedure has to be repeated for each iteration step. To obtain good initial values for the wavenumbers $k_\pm$ the model suggested by Dokumaci [20] for ducts with flow is used. Then using the TMM, the initial values of $\hat{p}_\pm$ are calculated.

When the unknown vector $\mathbf{y}$ is known one can calculate the reflection coefficient (R) at the reference microphone (No. 1) using Eq. (6) and transfer it to $x = 0$. The reflection coefficient at $x = 0\,(R_0)$ can be written as

$$R_0 = R\exp(\mathrm{i}(k_- + k_+)l), \tag{14}$$

where l is the distance from microphone 1 to the termination as shown in Fig. 2. This formula is used in Section 5 to determine the reflection properties of an unflanged pipe.

3. Description of measurement set-up

In order to test the full plane wave decomposition method described in Section 2, measurements were performed using the flow acoustic test facility available at The Marcus Wallenberg Laboratory [27]. A circular steel pipe of inner diameter 35 mm with a wall roughness of less than 1 μm, and outer diameter 40 mm was used. In the pipe six $\frac{1}{4}$ in microphones (B&K 4938) were flush mounted at the positions shown in Fig. 3. The first measurement position x_1 was fixed at 150 mm from the open end. At room temperature the cut-on frequency of the first higher-order mode in the test pipe is approximately 4.5 kHz.Two loudspeakers connected to the pipe via short side branches provided the acoustic excitation. The loudspeaker sections were placed in an anechoic room and a dissipative silencer was used to remove reflections from the upstream termination, together with a very smooth conical diffuser which also provided a low-noise inlet flow. The unflanged

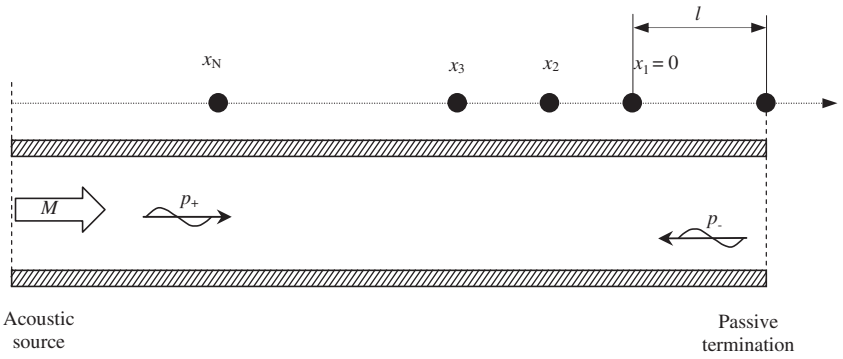

Fig. 2. Microphone positions used in the FWDM.

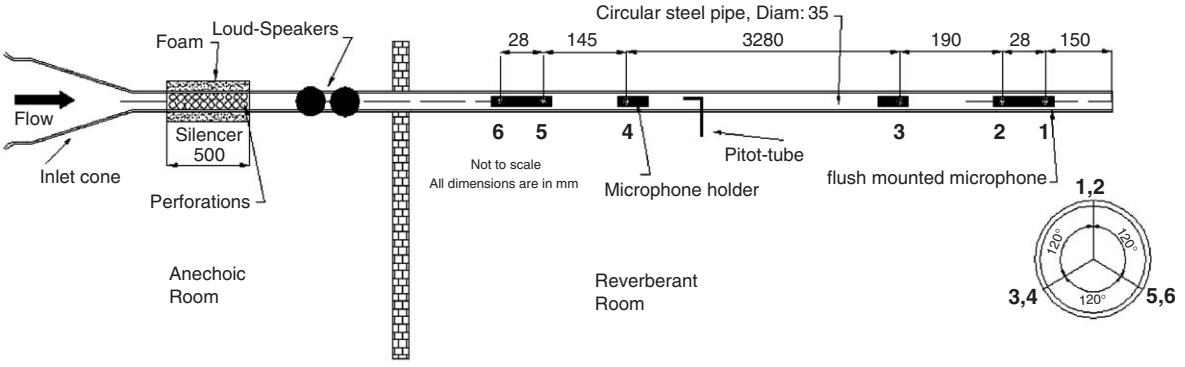

Fig. 3. Layout of the flow test rig at the Marcus Wallenberg Laboratory. The anechoic room is used as a pressure chamber which is driven by external fans and delivers a flow with a low acoustic noise level. Via the inlet cone and the test pipe the flow moves from the anechoic room to the reverberant room which is kept at atmospheric pressure.

opening of the pipe was placed in the middle of a reverberant room, 1.5 m above a rigid floor. The nearest wall was 2.4 m from the pipe open end. Careful attention was taken to avoid flow-induced vibrations of the pipe by using soft supports.

The microphones were flush-mounted and a source correlation technique [9] with stepped sine excitation was adopted to suppress the flow-generated noise and get a good signal-to-noise ratio. To improve the quality of the measurement the number of averages has been chosen to be between 400 and 1000. The measurements were repeated three times and the average values were used in the final analysis.

To obtain the flow speed a pitot-tube positioned in the middle of the cross-section was used, see Fig. 3. The average flow speed was obtained by assuming a fully developed turbulent flow. To calculate the speed of sound in the duct the temperature in the anechoic chamber (air at 20 °C) was used which is correct within $O(M^2)$. From the average flow speed and the speed of sound the Mach number was calculated. This was used to create an initial wavenumber estimate for the nonlinear solver. The experimentally determined Mach numbers were also used for plotting all the data. The tests with flow were performed up to Mach numbers around 0.3 but only data up to 0.2 are used for the results presented here as explained in the next paragraph.

The pressure drop along the duct will create a variation in the density which results in a variation of the flow speed along the duct. The Mach number and wavenumbers are therefore not exactly constant along the duct. This effect has been discussed earlier both by Ronneberger and Ahrens [23] and Peters [24]. For the pipe diameter used in our experiments it turns out that this effect gives an error less than 3% up to Mach numbers around 0.2.

3.1. Deviations from free field conditions at the pipe outlet

The influence of the rigid floor in the reverberation room on the reflection coefficient at the open end R_0 can be taken into account by assuming a mirror-image point source below the floor. The result is [28]

$$|R_{\mathrm{fl}}| - |R_0| = -\frac{(ka)^2}{4kH}\sin(2kH),$$
$$\delta_{\mathrm{fl}} - \delta = \frac{a^2}{8H}\cos(2kH), \tag{15}$$

where H is the distance from the pipe to the floor, a is the pipe radius, $|R_{\mathrm{fl}}|$ and δ_{fl} are the reflection coefficient magnitude and the end correction measured in the presence of the floor and R_0 and δ are the free field values. With the values $H = 1.5\,\mathrm{m}$ and $a = 0.0175\,\mathrm{m}$, Eq. (15) implies at the most 1% change for the reflection coefficient magnitude (high-frequency limit) and a negligible change for the end correction. In the results presented the data has been corrected for the floor reflections neglecting the effects of the other room surfaces as well as multiple reflections [24].

To validate and test the accuracy of the new full wave decomposition procedure the no flow case was used. Figs. 4 and 5 compare the reflection coefficient $|R_0|$ and the end correction represented as δ/a obtained for this case, with theoretical results of Levine and Schwinger [29]. It is found that the measured results agree within 1% with the theoretical predictions.

4. Propagation of plane waves in pipes

4.1. In the absence of mean flow

Kirchhoff [22] found that the propagation of sound waves in a pipe is dissipative because of visco-thermal losses at the pipe walls. His solution for a wide pipe shows that the wavenumber, $k = \omega/c_0$, is modified to kK_0, where the propagation constant K_0 is given by

$$K_0 = 1 + \frac{(1-\mathrm{i})}{\sqrt{2}s}\left(1 + \frac{(\gamma-1)}{\xi}\right) - \frac{\mathrm{i}}{s^2}\left(1 + \frac{\gamma-1}{\xi} - \frac{\gamma}{2}\frac{\gamma-1}{\xi^2}\right). \tag{16}$$

Here γ is the specific heat ratio, $\xi^2 = \mu C_p/\kappa_{\mathrm{th}}$ is the Prandtl number, $s = a\sqrt{\rho_0\omega/\mu}$ is the shear wavenumber, μ is the dynamic viscosity, κ_{th} is the thermal conductivity, C_p is the specific heat coefficient and a

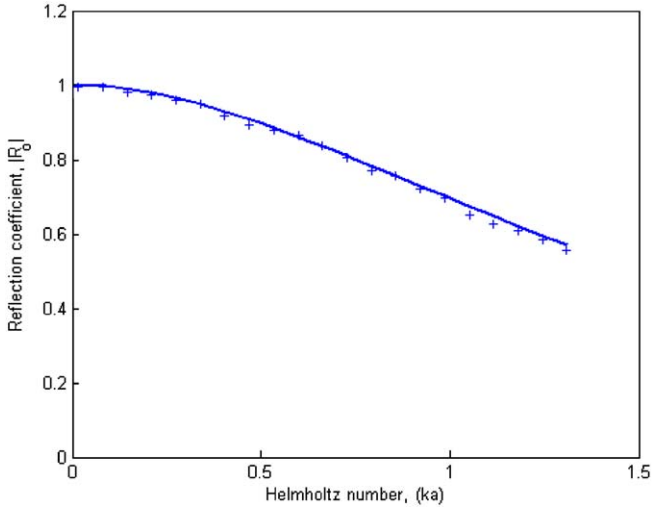

Fig. 4. Reflection coefficient magnitude versus Helmholtz number at $M = 0$ and $T = 293\,\mathrm{K}$: + + +, measured and —, predicted using Levine and Schwinger [29].

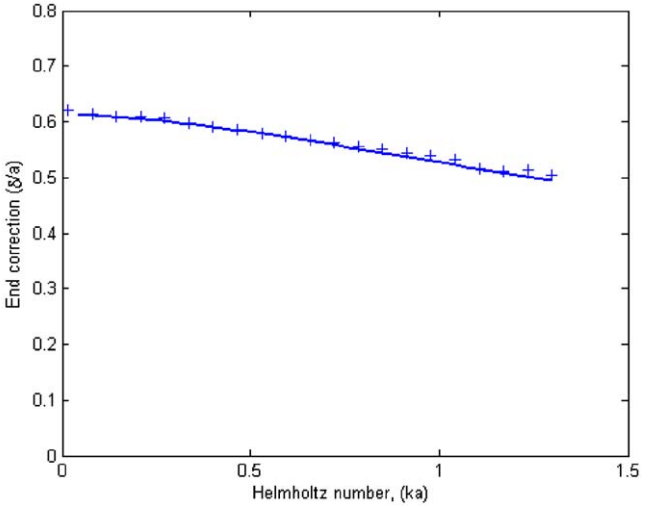

Fig. 5. End correction versus Helmholtz number at $M = 0$ and $T = 293\,\mathrm{K}$: $+++$, measured and —, predicted using Levine and Schwinger [29].

is the pipe radius. Kirchhoff's solution is valid for a homogenous medium in the absence of a mean flow. The damping in a quiescent fluid α_0 is given by the negative imaginary part of Eq. (16) multiplied by the wavenumber as

$$\alpha_0 = \frac{\omega}{c_0}\left(\frac{1}{\sqrt{2}s}\left(1+\frac{\gamma-1}{\xi}\right)+\frac{1}{s^2}\left(1+\frac{\gamma-1}{\xi}-\frac{\gamma}{2}\frac{\gamma-1}{\xi^2}\right)\right). \tag{17}$$

The s^{-2} term is very small and is usually neglected in the literature, see Pierce [30]. The visco-thermal losses in the fluid itself is given by Pierce [30] as

$$\alpha_{\mathrm{fluid}} = \frac{\omega}{c_0}\frac{(ka)^2}{2s^2}\left(\frac{4}{3}+\frac{\mu_b}{\mu}+\frac{\gamma-1}{\xi^2}\right), \tag{18}$$

where μ_b is the bulk viscosity which for air, is approximately 0.6μ. This contribution to the damping is two orders of magnitude smaller than the lossses at the walls and will be neglected.

4.2. The effect of convection

The mean flow speed U_0 influences the wavenumbers for up- and downstream propagating acoustic waves. In the literature a number of formulas and models have been presented to describe this effect and the aim of this section is to point out if these formulas and models agree with our experimental results. It can also be noted that there exist relatively few experimental validations for some of the existing formulas. The two most detailed are the works of Ronneberger and Ahrens [23] and Peters [24].

A one-dimensional ad hoc extension of the Kirchhoff solution [22] to the visco-thermal acoustic wave motion in a pipe carrying a uniform mean flow has been described by Davies et al. [16]. Davies argues that the propagation constant should be modified into

$$K^{\pm} = K_0/(1 \pm M), \tag{19}$$

where M denotes the (average) Mach number of the mean flow and K_0 is the classical Kirchoff solution. A theoretical solution to the problem of visco-thermal acoustic wave motion in pipes with flow has also been proposed by Dokumaci [20]. The solution is obtained by asymptotic expansion, for large shear wavenumbers $s \gg 1$ and small mean flow Mach numbers, of the solution of the convective acoustic equations simplified in the manner of the Zwikker and Kosten theory [21]. For the no flow case this solution is known to represent the

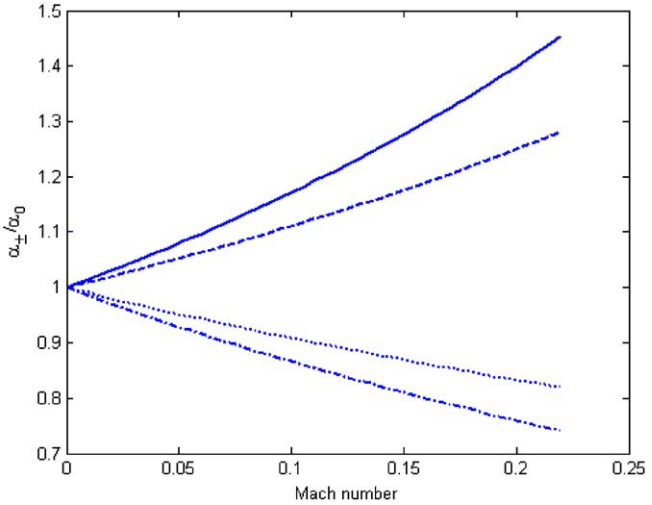

Fig. 6. Predicted α_-/α_0 by Dokumaci [20],— and by Davies [16], ---- at $ka = 0.0323$. Predicted α_+/α_0 by Dokumaci [20], -.-.-. and by Davies [16], · · · · · at $ka = 0.0323$.

full Kirchhoff solution accuratly for large shear wavenumbers. In this asymptotic theory the propagation constants are given by

$$K^{\pm} = K_0/(1 \pm K_0 M). \tag{20}$$

An example of the difference between the predicted damping from the two models for the pipe used in the test rig is shown in Figs. 6 and 7. As can be seen from these figures the difference between the two models can be more than 10% for high Mach numbers.

4.3. The effect of turbulence

In the presence of a turbulent flow the damping of the acoustic waves is influenced by the action of the turbulent stresses if the acoustic boundary layer thickness δ_{ac} is larger than that the viscous sublayer δ_l [23,24]. The acoustic boundary is defined as: $\delta_{ac} = \sqrt{2v/\omega}$ and the viscous sublayer of a turbulent pipe flow is defined as: $\delta_l \approx 10v/u_*$, where v is the kinematic viscosity, $u_* = \sqrt{\tau_w/\rho_0}$ is the friction velocity, τ_w is the wall shear stress and ρ_0 the fluid density. The effect of turbulence can be described in the first-order approximation by adding to the kinematic viscosity an eddy viscosity, which is non-uniform over the pipe cross-section. The eddy viscosity is small compared to the kinematic viscosity for distances from the wall (y) small compared to the thickness of sublayer δ_l. For $y > \delta_l$, i.e. in the logarithmic region of the turbulent boundary, the eddy viscosity increase approximately linear with the distance from the wall.

Ingard and Singal [18] have derived a quasi-stationary theory for the damping in the region where the acoustic boundary layers are much larger than the viscous sublayer. In practice, this implies a model valid for very low frequencies typically much less than 100 Hz.The wavenumbers can be calculated using

$$k_+ = \frac{k_0 - \mathrm{i}k'}{1 + M}, \text{ and } k_- = \frac{k_0 - \mathrm{i}k'}{1 - M}, \tag{21}$$

where $k_0 = 2\pi f/c$ and $k' = k'_v + k'_t$, represent the attentuation, the first part refer to the visco-thermal and the second refer to the turbulent effect. These attenuation terms are given by [18]

$$k'_v = \frac{1}{2D}\left(\frac{\mu\pi f}{\rho c^2}\right)^{1/2}\left[1 + \frac{(\gamma - 1)}{\xi}\right] \text{ and } k'_t = \frac{\Psi M}{2D}\left[1 + \frac{\Psi' Re}{2\Psi}\right] \tag{22}$$

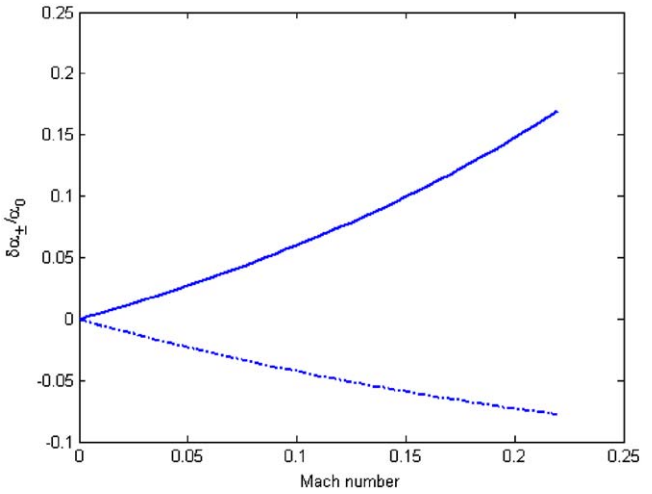

Fig. 7. —, differences $\delta\alpha_-/\alpha_0$ between Dokumaci [20] and Davies [16] at $ka = 0.0323$. -.-.-., differences $\delta\alpha_+/\alpha_0$ between Dokumaci [20] and Davies [16] at $ka = 0.0323$.

where D is the ratio between the duct cross-section area and its perimeter, Re is the Reynolds number, Ψ is the turbulent flow friction factor and $\Psi' = \partial\Psi/\partial Re$, which is a function of Reynolds number and defined as

$$\frac{1}{\sqrt{\Psi}} = 2\log_{10}\left(Re\sqrt{\Psi}\right) - 0.8. \tag{23}$$

The visco-thermal term in Eq. (22) is simply the damping from the classical Kirchhoff model and corresponds to the first term in Eq. (17). As discussed for instance by Peters et al. [24] the model of Ingard and Singhal [18] represents a very crude approximation, which also agrees poorly with available experimental data.

Peters et al. [24] proposed a modification of a rigid core model originally proposed by Ronneberger and Ahrens [23], by including a phase shift in the reflection of the shear waves which corresponds to a memory effect in the turbulent flow. The result they obtained is

$$\frac{\alpha_\pm}{\alpha_0} = \left(\frac{1+\exp\left(-2(1+\mathrm{i})\left(\delta_l/\delta_{\mathrm{ac}}\right) - 200\mathrm{i}\left(\delta_l/\delta_{\mathrm{ac}}\right)^2\right)}{\left(1-\exp\left(-2(1+\mathrm{i})\left(\delta_l/\delta_{\mathrm{ac}}\right)\right)\right)}\right)\left(\frac{1}{1\pm M}\right), \tag{24}$$

where $\delta_l \approx 12.5v/u_*$, $\delta_{\mathrm{ac}} = \sqrt{2v/\omega}$ and $u_* = \sqrt{\tau_w/\rho_0}$.

The most complete model developed so far is the one proposed by Howe [19]. This model is based on averaging the momentum and continuity equations over the cross-sectional area, A and use eddy viscosity to control the momentum and the thermal boundary layers. The model assumes that the thickness of these boundary layers is much smaller than the acoustic wavelength so that the layers can be described using an effective acoustic admittance. The resulting damping of the plane wave is given by

$$\alpha_\pm = \frac{\sqrt{2\omega}}{c_0 D_p(1\pm M)} Re\left\{\sqrt{2}\,\exp(-\mathrm{i}\pi/4)\left(\frac{\sqrt{v}}{(1\pm M)^2}\times F_A\left(\sqrt{\frac{\mathrm{i}\omega v}{\kappa_k^2 u_*^2}}, \delta_v\sqrt{\frac{\mathrm{i}\omega}{v}}\right)\right.\right.$$
$$\left.\left. + \frac{\beta c_0^2\sqrt{\chi}}{C_p}\times F_A\left(\xi^2\sqrt{\frac{\mathrm{i}\omega\chi}{\kappa_k^2 u_*^2}}, \delta_v\sqrt{\frac{\mathrm{i}\omega}{\chi}}\right)\right)\right\}, \tag{25}$$

where

$$F_A(a,b) = \frac{\mathrm{i}\left(H_1^1(a)\cos(b) - H_0^1(a)\sin(b)\right)}{H_0^1(a)\cos(b) + H_1^1(a)\sin(b)}, \tag{26}$$

$\chi = \kappa_{\text{th}}/\rho_0 C_p$, which for air at 20 °C is equal to 2×10^{-5} m^2/s, $\kappa_K \approx 0.41$, $\beta = 1/T$ and T is absolute temperature, $D_p = 4A/l_p$ is the hydraulic diameter, Re is the real part, H_J is the Hankel function of order J and the friction velocity is calculated from

$$U_0/u_* = 2.44 \ln\left(u_* D_p/2v\right) + 2.0. \tag{27}$$

The viscous sublayer (δ_v) in Eq. (25) is frequency dependent and is calculated from

$$\frac{\delta_v u_*}{v} = 6.5\left(1 + \frac{1.7\left(\omega/\omega_*\right)^3}{1 + \left(\omega/\omega_*\right)^3}\right), \quad \omega_* v/u_*^2 \approx 0.01 \quad \text{and } \omega > 0. \tag{28}$$

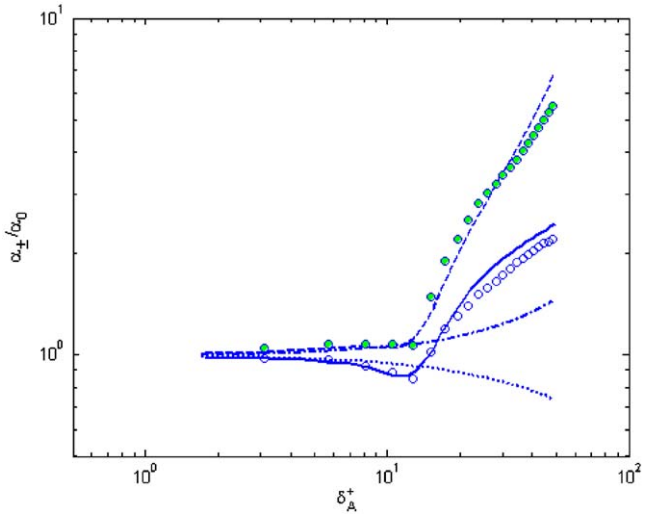

Fig. 8. Damping coefficient $\alpha_\pm/\alpha_0$ as a function of δ_A^+ at $ka = 0.0323$: ●●●, measured α_-/α_0, ----, predicted by Howe [19], -.-.-., predicted by Dokumaci [20]. ○○○, measured α_+/α_0, —, predicted by [19], · · · · ·, predicted by Dokumaci [20].

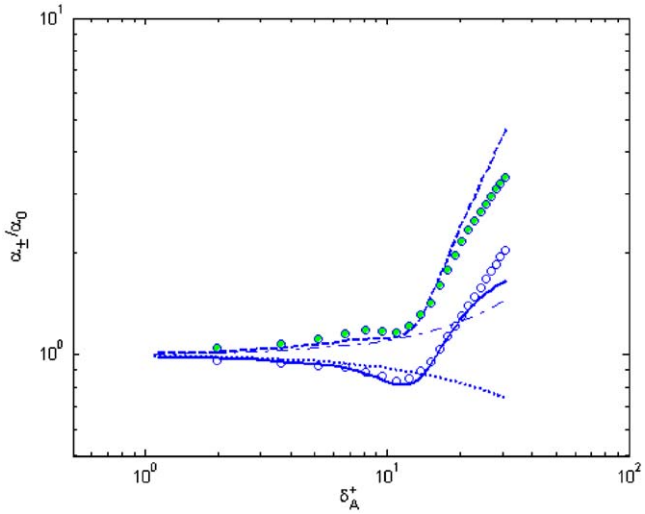

Fig. 9. Damping coefficient $\alpha_\pm/\alpha_0$ as a function of δ_A^+ at $ka = 0.0808$: ●●●, measured α_-/α_0, ----, predicted by Howe [19], -.-.-., predicted by Dokumaci [20]. ○○○, measured α_+/α_0, —, predicted by Howe [19], · · · · ·, predicted by Dokumaci [20].

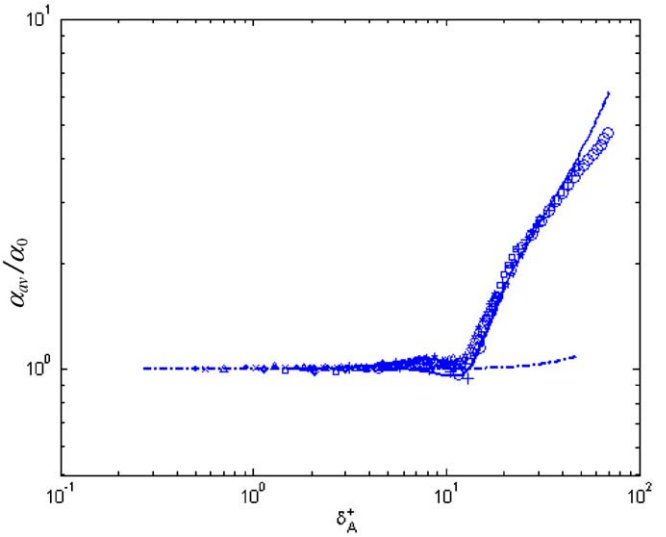

Fig. 10. Average damping coefficient α_{av}/α_0 as a function of δ_A^+: —, predicted by Howe [19] at $ka = 0.032$, -.-.-., predicted by Dokumaci [20] at $ka = 0.032$; ○○○, measured α_{av}/α_0 at $ka = 0.0162$, + + +, measured α_{av}/α_0 at $ka = 0.032$; ∗ ∗ ∗, measured α_{av}/α_0 at $ka = 0.0808$; □□□, measured α_{av}/α_0 at $ka = 0.1455$; ◇◇◇, measured α_{av}/α_0 at $ka = 0.2425$; △△△, measured α_{av}/α_0 at $ka = 0.3234$; ***, measured α_{av}/α_0 at $ka = 0.6468$; × × ×, measured α_{av}/α_0 at $ka = 0.9702$; ●●●, measured α_{av}/α_0 at $ka = 1.2936$.

In the next section the comparison between the measured and calculated damping coefficients ($\alpha_{\pm}$) and the average value, $\alpha_{av} = (\alpha_+ + \alpha_-)/2$ are presented, plotted versus the normalized boundary layer thickness $\delta_A^+ = \left(2u_*^2/v\omega\right)^{1/2}$.

4.4. Comparison with experimental data

In Figs. 8 and 9, the models of Howe [19] and Dokumaci [20] are compared with experimental data at a fixed frequency for varying Mach numbers. The data is collapsed by plotting against the normalized boundary layer thickness δ_A^+ [23,24]. As can be seen from the figures both models agree well with the data up to $\delta_A^+ \approx 10$. But Howe's model works well up to δ_A^+ values in the range 30–40. In Fig. 10, the average damping (sum of $+/-$) is presented. The conclusions are similar to what was said in relation to Figs. 8 and 9.

5. Sound reflection at an open end

This is a classical problem in acoustics that is important for instance for the radiation of sound from exhaust tailpipes. The classical solution to the problem of radiation from an unflanged open ended pipe into a free space was given by Levine and Schwinger [29]. This solution was later extended to include the effects of a mean flow by Munt [25]. The model of Munt has only been validated partly by the published experimental data and in particular accurate measurements of the phase of the reflection coefficient are lacking.

5.1. Effect of mean flow

In this section, the experimental results have been compared with the theoretical model presented by Munt [25] for the transmission of acoustic waves out of a semi-infinite circular pipe in the presence of subsonic flow out of the pipe. The model consists of a rigid circular pipe, with walls of negligible thickness; described by $r = a$ and $z \leqslant 0$ in cylindrical polar coordinates (r, θ, z), see Fig. 11. A gaseous jet of fluid is assumed to leave the pipe with a Mach number $M < 1$ and to be separated from the ambient gas, in $r > a$, by an infinitely thin vortex sheet occupying $r = a$, $z > 0$. The ambient gradient gas is taken to be flowing more slowly than the jet and in the same direction. The ratio of the speed of the ambient gas to that of the jet is denoted by η, so that

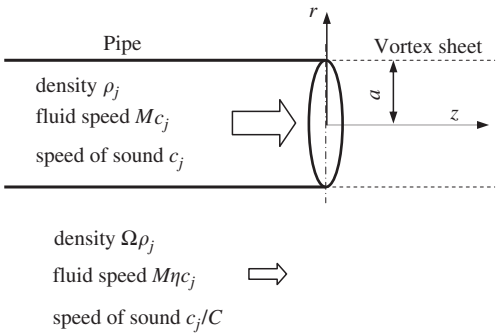

Fig. 11. Parameters used in the Munt [25] model.

$0 \leqslant \eta \leqslant 1$. Inside the jet fluid is taken to have density ρ_j, the speed of sound c_j and the fluid velocity Mc_j. Outside the jet fluid is taken to have density $\Omega\rho_j$, the speed of sound c_j/C and the fluid speed $M\eta c_j$.

Hence, the non-dimensional quantities η, Ω and C express the ratios of the mainstream value to the jet value for density, velocity and speed of sound, respectively.

The Munt solution is expressed in the form of integral equations which have been solved numerically in the presence of a uniform subsonic mean flow (plug flow) and for low acoustic amplitudes ($\hat{u}_{ac}/Mc_j \ll 1$) [31]. In the theory a Kutta condition (smooth separation at the trailing edge) is applied at the pipe opening, which implies a finite velocity and no pressure fluctuations at the edge. The Kutta condition implies that an acoustic disturbance in the jet can create a transfer of acoustic energy into kinetic energy in the jet vortex sheet. The Kutta condition also implies that the magnitude of the pressure reflection coefficient approaches a value of -1.0 for all Mach numbers if the Helmholtz number approaches zero, i.e.,

$$\lim_{ka \to 0} R_0 = -1 \quad \text{for all } M. \tag{29}$$

From the comparison between the experimental results and Munt's theory, better agreement is found when $|R_0|$ is calculated based on the maximum flow speed in the duct rather than the average. This can be argued based on the investigation by Freymuth [32] on the growth of disturbances at the outlet of a circular jet. In the Munt theory the convection speed of the vortical disturbances is $Mc_j/2$, assuming a zero flow on the outside as in the experiments. As shown by Freymuth in the real jet there is a distribution of vorticity which has a maximum at the position $r = a$, i.e., at the vortex sheet in the Munt model. The convection speed at this position is $U_{max}/2$ or half the maximum speed at $r = 0$. Since the interaction between the acoustic field and the convected vortical disturbances is an important part of Munts model, it is logical to choose the flow speed so that the correct vortex convection speed is preserved, i.e, to use U_{max} rather than the average flow speed for the comparison theory-measurement. All the results presented below is based on the maximum flow speed for the Munt's theory and average flow speed for the experimental data. Fig. 12 shows that there is a very good agreement between the predicted and measured data for the magnitude of the reflection coefficient especially at low Helmholtz-numbers ka. In Fig. 13 the same data is presented as a function of the Strouhal-number ($St = ka/M$). It can be noted that all curves have a maximum at the same St-number.

The boundary condition at an open end is for low frequencies always equal to zero acoustic pressure. This corresponds to a reflection coefficient of -1 and a phase of π. The end correction for an open end can then be defined as the necessary distance δ an open pipe has to be extended to create this low frequency limit value for the phase. The reflection coefficient at the opening can be written as $R_0 = |R_0| \exp(i\theta)$. Moving this a distance δ gives

$$R_\delta = |R_0| \exp[i(k_+ + k_-)\delta + i\theta]. \tag{30}$$

To create a phase angle equal to π the end correction δ becomes

$$\frac{\delta}{a} = \frac{\pi - \theta}{Re(k_+ + k_-)a} \approx \frac{(\pi - \theta)(1 - M^2)}{2ka}. \tag{31}$$

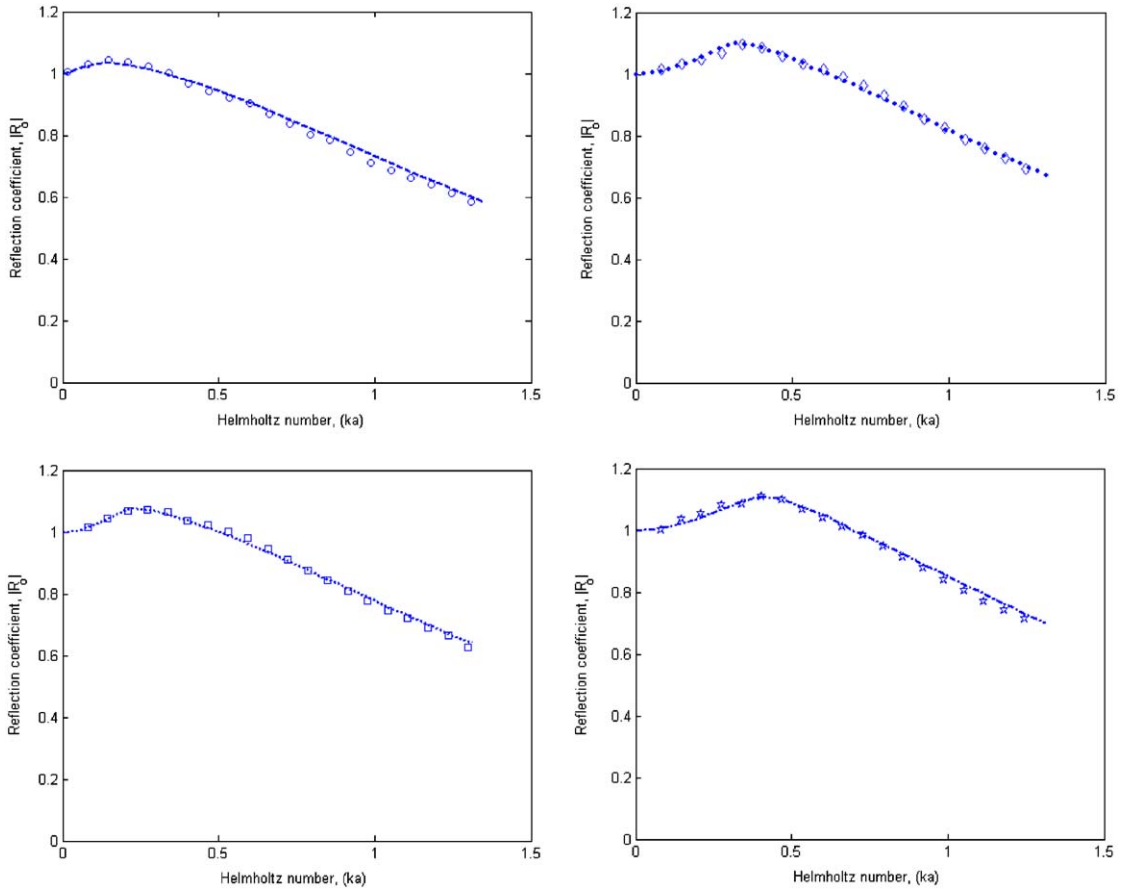

Fig. 12. Measured and predicted reflection coefficient magnitude at different at Helmholtz and Mach numbers: ○○○, measured at $M = 0.05$, ----, predicted at $M = 0.05$ by Munt [25]; □□□, measured at $M = 0.10$, ……, predicted at $M = 0.10$; ◇◇◇, measured at $M = 0.15$, ●●●●, predicted at $M = 0.15$ by Munt [25]; ***, measured at $M = 0.20$, -.-.-., predicted at $M = 0.20$ by Munt [25].

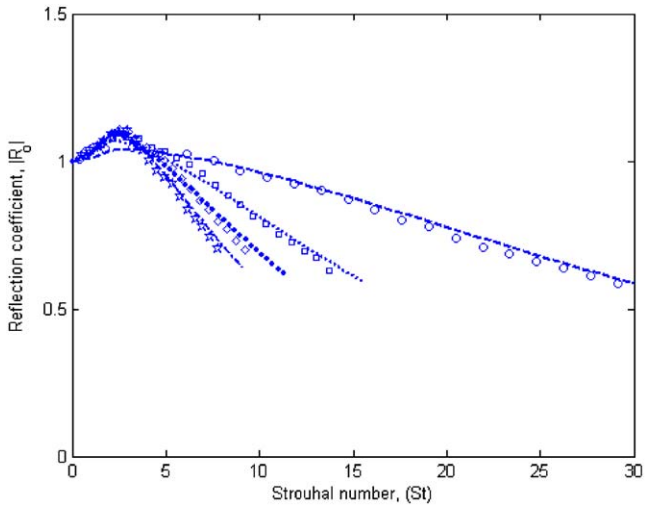

Fig. 13. Measured and predicted reflection coefficient magnitude at different Strouhal numbers: ○○○, measured at $M = 0.05$, ----, predicted at $M = 0.05$ by Munt [25]; □□□, measured at $M = 0.10$, ……, predicted at $M = 0.10$ by Munt [25]; ◇◇◇, measured at $M = 0.15$, ●●●●, predicted at $M = 0.15$ by Munt [25]; ***, measured at $M = 0.20$, -.-.-., predicted at $M = 0.20$ by Munt [25].

Rienstra [33] found a discontinuous behaviour of the end correction. For low frequencies ka, when $M = 0$ the end correction attains the same value as found by Levine and Schwinger [29], i.e.,

$$\lim_{M=0,ka\to 0} \delta/a = 0.6133. \tag{32}$$

But for any positive $M \ll 1$ Rienstra [33] found

$$\lim_{ka\to 0} \delta/a = 0.2554\sqrt{1-M^2}. \tag{33}$$

Concerning earlier measurements of an open end with flow Davies et al. [16] report that with flow present, the value of the end correction might be reduced at very low Helmholtz numbers. But the measurements were

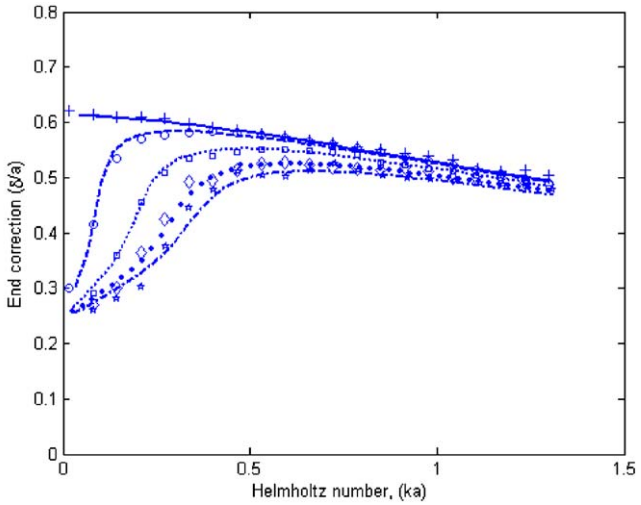

Fig. 14. Measured and predicted end correction at different Helmholtz and Mach number: + + +, measured at $M = 0$, —, predicted at $M = 0$ by Levine and Schwinger [29]; ○○○, measured at $M = 0.05$, ----, predicted at $M = 0.05$ by Munt [25]; □□□, measured at $M = 0.10$, ….., predicted at $M = 0.10$ by Munt [25]; ◇◇◇, measured at $M = 0.15$, ●●●●, predicted at $M = 0.15$by Munt [25]; ***, measured at $M = 0.20$, -.-.-., predicted at $M = 0.20$ by Munt [25].

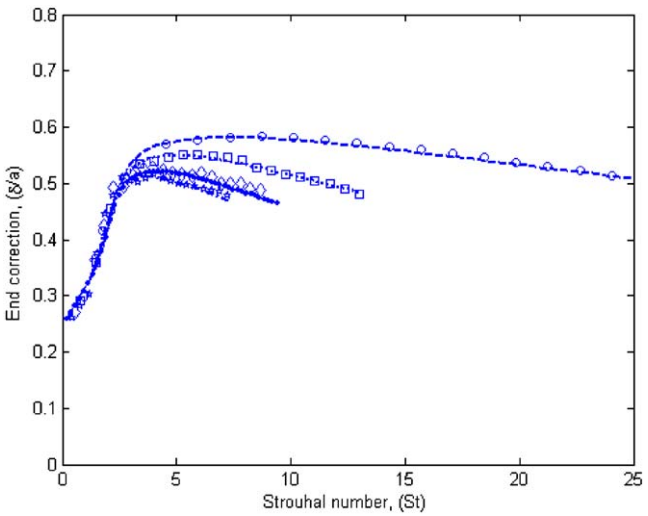

Fig. 15. Measured and predicted end correction at different Strouhal numbers: ○○○, measured at $M = 0.05$, ----, predicted at $M = 0.05$ by Munt [25]; □□□, measured at $M = 0.10$, ….., predicted at $M = 0.10$ by Munt [25]; ◇◇◇, measured at $M = 0.15$, ●●●●, predicted at $M = 0.15$ by Munt [25]; ***, measured at $M = 0.20$, -.-.-., predicted at $M = 0.20$ by Munt [25].

not conclusive since they did not cover this range adequately. Therefore, the conclusion was that the effect is small and can be neglected, i.e., that the no flow value can be used. The data presented here together with the low-frequency data of Peters et al. [24] clearly show that the end correction is strongly reduced at low Helmholtz and Strouhal numbers and that the limit suggested by Rienstra [33] seems correct.

In Figs. 14 and 15, the theoretical prediction using the maximum flow speed in the pipe is compared with the experimental data. It is clear from the comparison that there is a very good agreement between the measured and predicted data.

The end correction is strongly affected by the flow at low Helmholtz numbers. The lowest measured limit for the magnitude of the reflection coefficient is 1.005 at $ka = 0.0162$ and the lowest limit for the end correction is 0.265 at $St = 0.15$, which is close to the value predicted by Rienstra [33]. It can also be noted that with increasing Helmholtz number the end correction values move toward the no flow case as can be seen from Fig. 14.

6. Summary and conclusions

A new full plane wave decomposition method that determines both wave amplitudes and wavenumbers from measured acoustic pressures using an array of microphones is suggested. The formalism for the new method is developed and then the method is applied to study the effect of flow on damping of plane waves and on the reflection of sound from an unflanged open pipe termination. With respect to the damping it has been fund that Dokumaci's model [20] can be used when $\delta_A^+ < 10$ and Howe [19] can be used up to $\delta_A^+ \approx 30$–40. Concerning the reflection from an open end it has been found that the theory of Munt [25] combined with the maximum flow speed rather than the average, gives a very good agreement with the measured results. To continue this study measurements at higher Mach numbers are of interest. Here, the maximum value used in the analysis was around 0.20. Experimental tests of the Munt theory [25] with hot gases or two gases with different acoustic properties are also of interest.

Acknowledgments

The authors would like to thank Professor S. W. Rienstra and Peter in't Panhuis (M.Sc.), at Eindhoven University of Technology, Netherlands for providing the coded version of Munt's theory. The work in the paper is performed within the ARTEMIS project; funded by the EC (European commission), Contract No. G3RD-CT-2001-00511. Dr. Susann Boij is also acknowledged for useful discussions.

References

[1] ISO 10534-1, Acoustics—Determination of Sound Absorbing Coefficient and Impedance in Impedance Tubes, Part I: Method Using Standing Wave Ratio, 1996.
[2] ISO 10534-2, Acoustics—Determination of Sound Absorption coefficient and Impedance method in Impedance Tubes, Part II: Transfer–Function method, 1998.
[3] V.B. Panicker, M.L. Munjal, Impedance tube technology for flow acoustics, *Journal of Sound and Vibration* 77 (4) (1981) 573–577.
[4] W.T. Chu, Impedance tube measurements—comparative study of current practices, *Noise Control Engineering Journal* 37 (1991) 37–41.
[5] W.T. Chu, Further experimental studies on the transfer function technique for the impedance tube measurements, *Journal of Acoustical Society of America* 83 (1988) 2225–2260.
[6] J.Y. Chung, D.A. Blaser, Transfer function method of measuring in-duct acoustic properties, I: theory, *Journal of Acoustical Society of America* 68 (1980) 907–913.
[7] J.Y. Chung, D.A. Blaser, Transfer function method of measuring in-duct acoustic properties, II: experiment, *Journal of Acoustical Society of America* 68 (1980) 914–921.
[8] H. Bodén, M. Åbom, Influence of errors on the two microphone method for measuring acoustic properties in ducts, *Journal of Acoustical Society of America* 79 (2) (1986) 541–549.
[9] M. Åbom, H. Bodén, Error analysis of two-microphone measurements in duct with flow, *Journal of Acoustical Society of America* 83 (1988) 2429–2438.
[10] F. Seybert, B. Soenarko, Error analysis of spectral estimates with application to the measurement of acoustic parameters using random sound fields in ducts, *Journal of Acoustical Society of America* 69 (1981) 1190–1199.

[11] M.L. Munjal, A.G. Doige, The two-microphone method incorporating the effects of mean flow and acoustic damping, *Journal of Sound Vibration* 137 (1990) 135–138.
[12] T. Fujimori, S. Sato, H. Miura, An automated measurement system of complex sound pressure reflection coefficients, *Proceedings of Inter Noise* 84 (1984) 1009–1014.
[13] J. Pope, Rapid measurement of acoustic impedance using a single microphone in a standing wave tube, *Proceedings ICA* 12, Paper M3-3, 1986.
[14] M.G. Jones, T.L. Parrott, Evaluation of a multi-point method for determining acoustic impedance, *Mechanical System and Signal Processing* 3 (1989) 15–35.
[15] S.-H. Jang, J.-G. Ih, On the multiple microphone method for measuring in-duct acoustic properties in the presence of mean flow, *Journal of Acoustical Society of America* 103 (3) (1998) 1520–1526.
[16] P.O.A.L. Davies, M. Bhattacharya, J.L. Bento Coelho, Measurement of plane wave acoustic fields in flow ducts, *Journal of Sound and Vibration* 72 (4) (1980) 539–542.
[17] M.L. Munjal, *Acoustic of Ducts and Mufflers*, Wiley Interscience, New York, 1987.
[18] U. Ingard, V.K. Singhal, Sound attenuation in turbulent pipe flow, *Journal of Acoustical Society of America* 55 (1974) 535–538.
[19] M.S. Howe, The damping of sound by wall turbulent sheer layers, *Journal of Acoustical Society of America* 98 (3) (1995) 1723–1730.
[20] E. Dokumaci, A note on transmission of sound in a wide pipe with mean flow and viscothermal attenuation, *Journal of Sound and Vibration* 208 (4) (1997) 653–655.
[21] E. Dokumaci, Sound transmission in narrow pipes with superimposed uniform mean flow and acoustic modeling of automobile catalytic converters, *Journal of Sound and Vibration* 182 (1995) 799–808.
[22] G. Kirchhoff, Uber den einfluss der wärmteleitung in einem gas auf die schallbewegung, *Annalen der Physik* 134 (6) (1868) 177–193.
[23] D. Ronneberger, C.D. Ahrens, Wall shear stress caused by small amplitude perturbations of turbulent boundary-layer flow: an experimental investigation, *Journal of Fluid Mechanics* 83 (4) (1977) 433–464.
[24] M.C.A.M. Peters, A. Hirsschberg, A.J. Reijnen, A.P.J. Wijnands, Damping and reflection coefficient measurements at low mach and low Helmholtz numbers, *Journal of Fluid Mechanics* 265 (1993) 499–534.
[25] R.M. Munt, Acoustic transmission properties of a jet pipe with subsonic jet flow, I: the cold jet reflection coefficient, *Journal of Sound and Vibration* 142 (3) (1990) 413–436.
[26] G. Dahlquist, Å. Björck, N. Anderson, *Numerical Methods*, Prentice-Hall, Englewood Cliffs, NJ, 1974.
[27] S. Allam, Acoustic Modelling and Testing of Advanced Exhaust System Components for Automotive Engines. Ph.D Thesis, Paper I, 2004.
[28] J.H.M. Disselhorst, L. Van Wijngaarden, Flow in the exit of open pipes during acoustic resonance, *Journal of Fluid Mechanics* 99 (2) (1980) 293–319.
[29] H. Levine, J. Schwinger, On the radiation of sound from an unflanged circular pipe, *Physical Review* 73 (1948) 383–406.
[30] A. Pierce, *Acoustics—An Introduction to its Physical Principles and Applications*, Mc Graw-Hill, New York, 1981.
[31] P. Panhuis, Calculations of the Acoustic End Correction of a Semi-Infinite Circular Pipe Issuing A Subsonic Cold or Hot Jet with Co-Flow, MSc Thesis, November 2003, Stockholm, Sweden, 2003.
[32] P. Freymuth, On transition in a separated laminar boundary layer, *Journal of Fluid Mechanics* 25 (1965) 683–704.
[33] S.W. Rienstra, A small Strouhal number analysis for acoustic wave–jet flow-pipe interaction, *Journal of Sound and Vibration* 86 (4) (1983) 539–556.